

Preparation of undoped and Tb³⁺-doped fluorescent HfO₂ spherical particles

Tomoe SANADA, Masashi KAWAI, Hiroshi NAKASHITA, Taichi MATSUMOTO, Noriyuki WADA* and **Kazuo KOJIMA†**

Department of Applied Chemistry, College of Life Sciences, Ritsumeikan University, 1-1-1, Noji-Higashi, Kusatsu, Shiga 525-8577
***Department of Materials Science and Engineering, Suzuka National College of Technology, Shiroko-cho, Suzuka 510-0294**

Undoped and Tb³⁺-doped HfO₂ spherical particles were prepared by a sol-gel method, by using hafnium tetra-*t*-butoxide (Hf(O-*t*-C₄H₉)₄) as a precursor of hafnium dioxide, SPAN85® as a surfactant, mixed solvent of C₂H₅OH and *n*-C₄H₉OH, and H₂O, followed by investigation of their structural and optical properties. Spherical particles with good morphology and comparatively high dispersibility were obtained from solutions with the molar ratio SPAN85®:H₂O = 1:8–17.5, their sizes being 0.2–5 μm in diameter. Particles became small and aggregated when the molar ratio of H₂O was more than 17.5, but became large when it was less than 8. Spherical particles heat treated at 400°C or below were amorphous, and those heat treated at 600°C or above were crystallized. Tb³⁺-doped HfO₂ spherical particles showed green luminescence due to the ⁵D₄→⁷F_J (J = 6, 5, 4, 3) transitions of the Tb³⁺ ion, and relatively strong luminescence was observed both in dried gel particles and particles heat treated at 1000°C. These Tb³⁺-doped HfO₂ spherical particles can be expected for new optical materials.

©2008 The Ceramic Society of Japan. All rights reserved.

Key-words : Spherical particle, Hafnium dioxide, Sol-gel method, Terbium, Luminescence

[Received June 11, 2008; Accepted October 16, 2008]

1. Introduction

Spherical particle phosphors of small sizes may be packed easily to produce various types of high-resolution optical displays and panels, and are therefore expected as new phosphors. The Tb³⁺ ion is the typical rare earth ion showing green luminescence. Therefore, Tb³⁺-doped spherical particles can be expected for applications in green spherical-particle phosphors.

HfO₂ has low phonon energy (about 780 cm⁻¹)^{1,2)} and is considered to be a host material suitable for luminescence of rare earth ions. HfO₂ is the substance with high hardness, high permittivity and large band gap, therefore, it is technically important for new generation materials. Compared with zirconium dioxide ZrO₂ which has similar structural features, HfO₂ has low thermal expansion coefficient³⁾ and high phase transition temperatures: monoclinic to tetragonal (1720°C), tetragonal to cubic (2600°C), and cubic to liquid (2800°C).⁴⁾

Especially, tetragonal HfO₂ has the outstanding hardness and high chemical stability comparable as a diamond, and the high density of HfO₂ when crystallizing to tetragonal is suitable for host lattice of rare earth ions, and is attractive for a scintillating substance.⁵⁾ There have been some reports on optical properties of HfO₂ doped with transition metal ions such as Mn²⁺, Eu³⁺, Tb³⁺, Sm³⁺, and Ce³⁺ ions.⁶⁾⁻¹⁰⁾

The preparation of HfO₂ particles by hydrothermal method has been reported.¹¹⁾⁻¹³⁾ Spherical particles of amorphous HfO₂ have been prepared by hydrolysis of hafnium-*t*-butoxide both in the aerosol phase and in ethanolic solutions.³⁾ Moreover, uniform elongated colloidal HfO₂ particles have been fabricated.¹⁴⁾

To our knowledge, there have been no reports on the prepara-

tion and properties of HfO₂ spherical particles doped with rare earth ions such as Tb³⁺. In the present study, we first established a sol-gel preparation method of undoped HfO₂ spherical particles, and then produced Tb³⁺-doped HfO₂ spherical particles by applying this method. Structural and luminescence properties of the particles were investigated.

2. Experimental procedure

Undoped and Tb³⁺-doped HfO₂ spherical particles were prepared by a sol-gel method. A starting solution consisted of hafnium tetra-*t*-butoxide (Hf(O-*t*-C₄H₉)₄) as a precursor of hafnium dioxide, sorbitan trioleate (C₆₀H₁₀₈O₈; SPAN85®, available from ICI America's Inc.) as a surfactant, H₂O, and C₂H₅OH and *n*-C₄H₉OH as solvents, with the molar ratio Hf(O-*t*-C₄H₉)₄:SPAN85®:H₂O:C₂H₅OH:*n*-C₄H₉OH = 1:0.01–1:2–10:22:55.

Undoped particles were prepared as follows: C₂H₅OH, *n*-C₄H₉OH, SPAN85® and H₂O were mixed and stirred for 15 min to prepare a solution. Hf(O-*t*-C₄H₉)₄ was added into the mixed solvent of C₂H₅OH and *n*-C₄H₉OH under N₂ atmosphere to prepare another solution. These two solutions were mixed with stirring for 30 min in the air, and then kept for 24 h. Tb³⁺-doped HfO₂ particles of the system 1Tb₂O₃·99HfO₂ were prepared by the same method, except for dissolving Tb(C₅H₇O₂)₃·H₂O into the former solution containing SPAN85® described above. Gel powders prepared in the solution were filtered with suction and washed with C₂H₅OH, followed by drying at 100°C for 24 h to obtain dried gel powders. The heat treatment was carried out for the dried gel powders at 200–1000°C in the air.

The morphology and particle size of spherical particles were measured with a scanning electron microscope (SEM: KEYENCE VE-8800) and a field emission scanning electron microscope (FE-SEM: Hitachi S-4800). IR spectra were taken

† Corresponding author: K. Kojima; E-mail: kojimaka@sk.ritsumei.ac.jp

on a Fourier transform infrared spectrometer (FT-IR: Shimadzu FT-IR 8600). X-ray diffraction (XRD) patterns were measured with an X-ray diffractometer (Rigaku RINT-2200) with Cu K α radiation. Luminescence and excitation spectra were recorded on a fluorescence spectrometer (Hitachi F-4500) with an Xe lamp as an excitation source. Luminescence quantum yield (QY) values were obtained by an absolute photoluminescence quantum yield measurement system (Hamamatsu C9920-02), under excitation at 254 nm with an Xe lamp as an excitation source. X-band ESR spectra were recorded on an instrument (JEOL FE2XG) at room temperature.

3. Results and discussion

Samples were prepared by changing the molar ratios of SPAN85® and H₂O with respect to Hf(O-t-C₄H₉)₄ in starting solutions. The molar ratios of C₂H₅OH and n-C₄H₉OH have been constant in all samples.

The relation between the molar ratios in the starting solutions and the morphology of undoped HfO₂ dried gel particles is summarized in **Fig. 1**. The marks indicate different types of particles obtained: ● (good spherical particles), ▲ (spherical and bulky particles), and ■ (bulky and aggregated particles).

Figure 2 shows SEM photographs of dried gel particles of undoped HfO₂ prepared from starting solutions with various molar ratios. In comparison of Figs. 2(a) with 2(b), where the

molar ratio of Hf(O-t-C₄H₉)₄ in the starting solution was doubled, it is found that aggregation of particles decreases and the particle size becomes large. In comparison of Fig. 2(c) and 2(d), where the molar ratio of H₂O in the starting solution was dou-

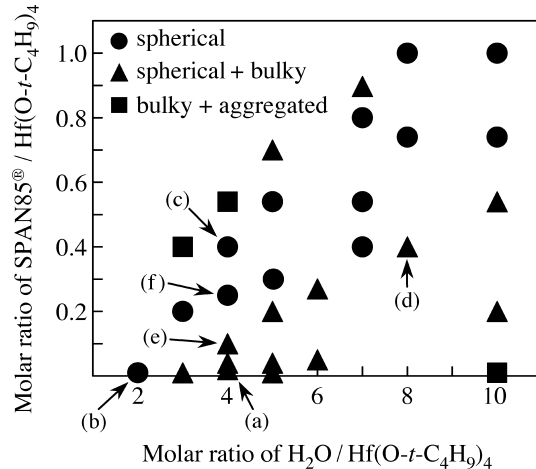


Fig. 1. Relationship between the molar ratio of starting solution and morphology of HfO₂ dried gel particles. Samples (a)–(f) correspond to those in Fig. 2 below.

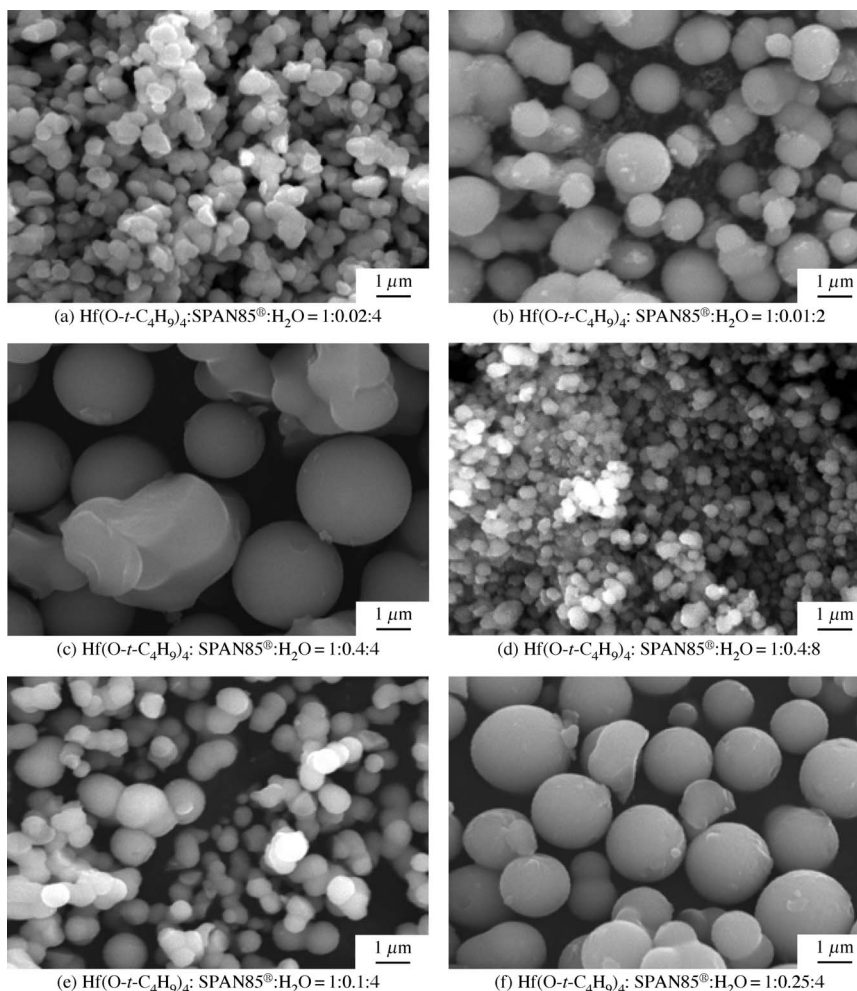


Fig. 2. SEM photographs of HfO₂ dried gel particles prepared from starting solutions with various molar ratios of starting materials.

bled, aggregation of particles increased and the particle size became small. Comparing Figs. 2(e) with 2(f), where the molar ratio of SPAN85® in the starting solution was changed by a factor of 2.5, aggregation of particles decreased and the particle size became large.

Spherical particles with good morphology and dispersion were obtained from the starting solutions with the molar ratios of H₂O/SPAN85® = 8–17.5; the most favorable spherical particles were obtained with the molar ratio Hf(O-t-C₄H₉)₄:SPAN85®:H₂O = 1:0.25:4, as shown in Figs. 1(f) and 2(f).

The effect of SPAN85® for obtaining good spherical particles is considered to be as follows: when a large excess of SPAN85® is used, the viscosity of sol solution increases enormously, leading to less dispersion and inhomogeneous concentration of Hf(O-t-C₄H₉)₄. As a result, it is likely that particles of large size are obtained, and aggregation occurs. As the concentration of SPAN85® is too low, the viscosity of sol solution decreases, which results in collisions of small particles to lead to aggregation before the precursor particle growth. When appropriate concentrations of SPAN85® are used, as shown in Fig. 1, molecules of SPAN85® cover the surface of the spherical particles considerably, and then the precursor particles can grow maintaining the spherical shape without aggregation.

Figure 3 shows heat-treatment effects of XRD patterns for undoped HfO₂ spherical particles prepared from the starting solution with the molar ratio Hf(O-t-C₄H₉)₄:SPAN85®:H₂O = 1:0.25:4. It is found that cubic HfO₂ dominates in the spherical

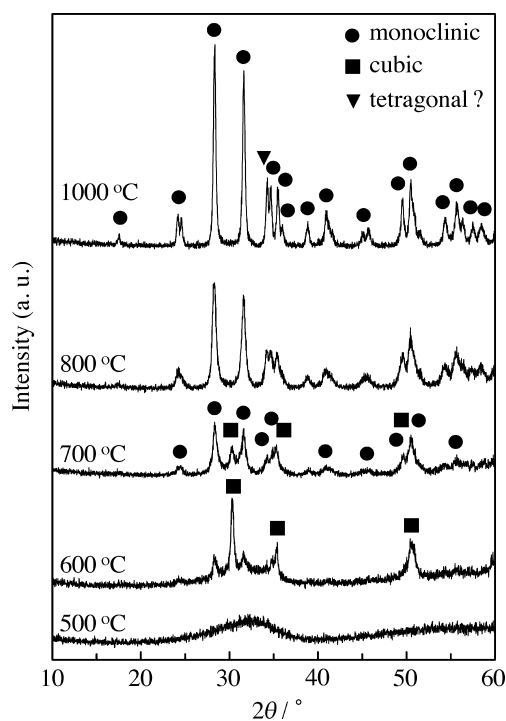


Fig. 3. XRD patterns of undoped HfO₂ spherical particles heat treated at various temperatures.

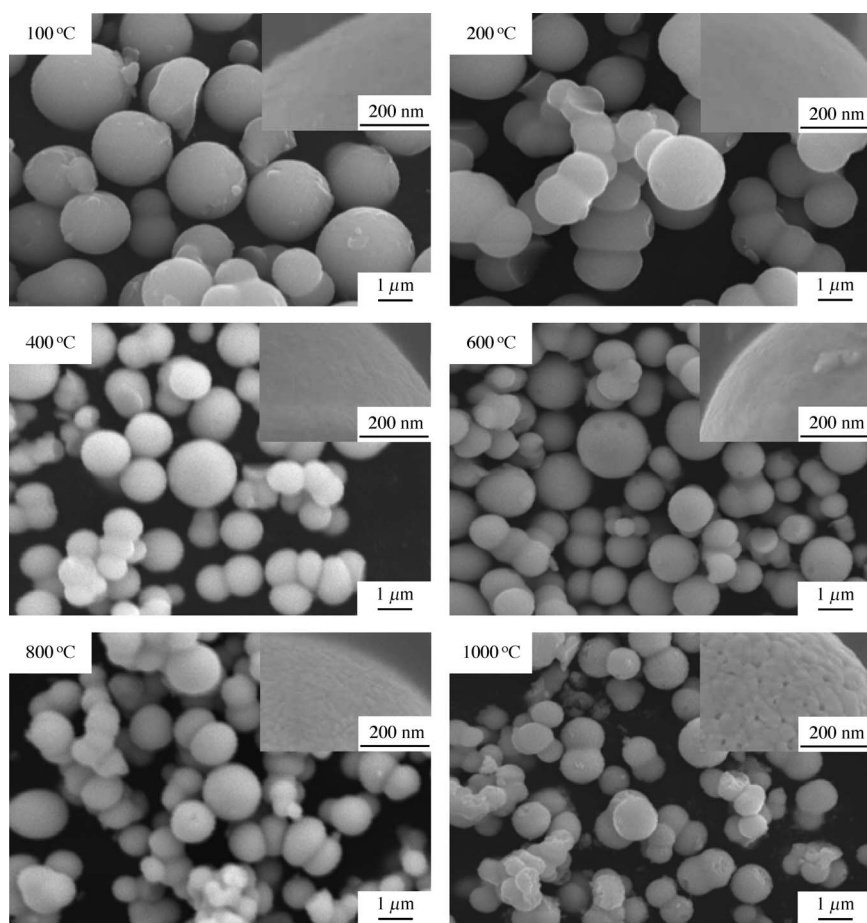


Fig. 4. SEM photographs of undoped HfO₂ spherical particles heat treated at various temperatures. Insets are FE-SEM photographs of surfaces of the particles.

particles heat treated at 600°C, cubic and monoclinic HfO₂ phases coexist in those heat treated at 700°C, and monoclinic HfO₂ becomes dominant in those heat treated at 800°C or above. Moreover, weak diffraction peaks, considered to be due to tetragonal HfO₂, are observed in the spherical particles heat treated at 1000°C. Similar diffraction peaks have also been observed in rare earth-doped yttrium-hafnium sol-gel oxide powders heat treated at 1000°C.⁶⁾ Usually, monoclinic HfO₂ was obtained by the heat treatment at lower temperatures such as several hundred °C,^{4),13),15),16)} while it is considered that tetragonal HfO₂ becomes dominant by the heat treatment at 1000°C or above, and by adding Y₂O₃ into HfO₂.⁶⁾ Cubic HfO₂ as well as monoclinic HfO₂ were observed in the spherical particles heat treated at 600 and 700°C. As described in the section of Introduction, cubic HfO₂ can be obtained by phase transition from tetragonal HfO₂ at the high temperature of about 2600°C.⁴⁾ It is thermodynamically metastable at low temperatures, and therefore seems to appear only under special conditions like ion beam assisted deposition at low temperatures.¹⁷⁾ Since cubic HfO₂ is attractive as high dielectric constant material, preparing cubic HfO₂ by such a simple sol-gel method in the present study will be of value.

Figure 4 shows SEM photographs of undoped HfO₂ spherical

particles heat treated at various temperatures. These particle sizes were about 1 μm in diameter, and the sizes decreased and surfaces of the spherical particles became coarse with increasing the heat-treatment temperature. Especially, it is found that surfaces of the spherical particles heat treated at 800 and 1000°C are quite coarse with some hollows. This is probably caused by burning out of residual organics and by densification of the spherical particles with the surface grain growth during the heat treatment at high temperatures. Similar coarsening has been reported for Co₃O₄ particles prepared from cobalt alkoxides.¹⁸⁾

SEM photographs of 1Tb₂O₃-99HfO₂ samples, dried (100°C) gels and spherical particles heat treated at 1000°C, are shown in **Fig. 5**. These doped particles are found to be spherical, however their morphology is somewhat inferior to the undoped HfO₂ spherical particles.

Figure 6 shows luminescence and excitation spectra of 1Tb₂O₃-99HfO₂ spherical particles heat treated at various temperatures. Under UV excitation at 254 nm, green luminescence due to the ⁵D₄ → ⁷F_J (*J* = 6, 5, 4, 3) transitions of Tb³⁺ ions was observed (Fig. 6(a)). The luminescence was strong in the dried gel particles (*QY* = 1.3 ± 0.1%) and the spherical particles heat treated at 1000°C (*QY* = 0.9 ± 0.1%).

Some investigations for optical properties of rare earth ions

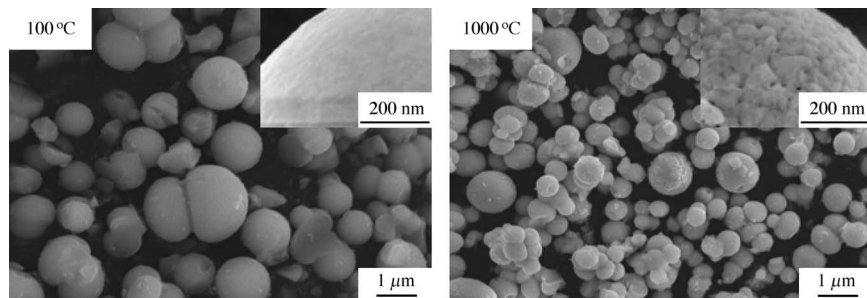


Fig. 5. SEM photographs of 1Tb₂O₃-99HfO₂ dried (100°C) gels and spherical particles heat treated at 1000°C. Insets are FE-SEM photographs of surfaces of the particles.

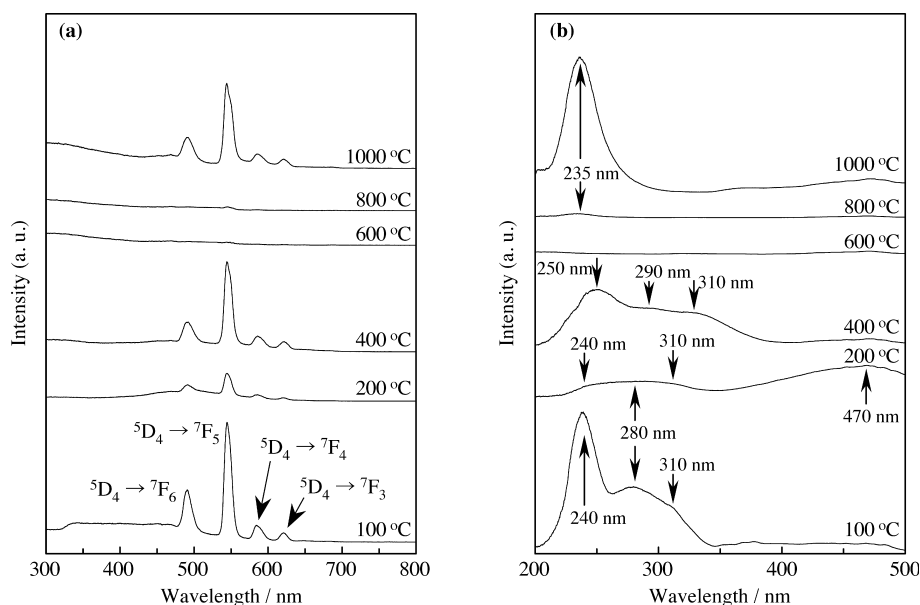


Fig. 6. Luminescence spectra (a) under excitation at 254 nm and excitation spectra (b) for the 545-nm luminescence of 1Tb₂O₃-99HfO₂ spherical particles heat treated at various temperatures.

doped in HfO_2 have been reported, as mentioned in the section of Introduction. The relation between the luminescence intensity and the heat-treatment temperature has been reported in Ce^{3+} -doped HfO_2 materials.^{10),19)} In monoclinic HfO_2 layers heat treated at 300–500°C, the luminescence due to Ce^{3+} ions weakens with increasing the heat-treatment temperature,¹⁰⁾ while in strontium hafnate powders containing orthorhombic SrHfO_3 and monoclinic HfO_2 that were heat treated at 800–1200°C, the Ce^{3+} ion showed the strongest luminescence in a sample heat treated at the high temperature of 1200°C.¹⁹⁾ These results somewhat resemble the result in the present study; the Tb^{3+} ion showed strong luminescence both in the samples heat treated at low temperatures and in the monoclinic HfO_2 spherical particles heat treated at 1000°C.

The reason why the luminescence intensity of the Tb^{3+} ion is low in the monoclinic HfO_2 spherical particles heat treated at 600 and 800°C is that the particles heat treated at 600°C are dark brown-colored due to residual carbon species resulted from combustion of organics during the heat treatment and that the crystallinity of the spherical particles heat treated at 800°C is incomplete. The oxidation of Tb^{3+} ions to Tb^{4+} ions has been reported to occur in oxide samples during the heat treatment, and those Tb^{4+} ions have been detected by optical absorption²⁰⁾ and ESR^{21),22)} spectra. In the present study, no XRD data for mixed oxides like Tb_4O_7 containing Tb^{3+} and Tb^{4+} ions were obtained, and no ESR signal due to Tb^{4+} ions were obtained, therefore the oxidation of Tb^{3+} ions is not likely to occur. In addition, an ESR signal with g value of about 2.002 which is due to carbon-related radicals^{23),24)} was observed in the spherical particles heat treated at 200, 400 and 600°C, where the dark brown spherical particles heat treated at 600°C had the strongest intensity.

Figure 6(b) shows excitation spectra of $1\text{Tb}_2\text{O}_3\cdot99\text{HfO}_2$ spherical particles heat treated at various temperatures. All of the excitation bands and shoulders observed in the range of 240 to 350 nm are probably due to the $4f^8$ to $4f^75d^1$ transitions of Tb^{3+} .^{25),26)} No band gap transition in HfO_2 may appear in Fig. 6(b) because of its large band gap energy of 6.15 eV (201 nm).²⁷⁾ According to the previous report,²⁸⁾ the peaks and shoulders observed in Fig. 6(b) are considered to be due to Tb^{3+} -containing small-size particles (235 and 240 nm) and agglomerated particles (280, 290, 310 and 330 nm).

As mentioned above, both the doped dried gel particles and the spherical particles heat treated at 1000°C are found to be favorable for the Tb^{3+} luminescence in the present study. Further study will be needed to produce Tb^{3+} -doped HfO_2 spherical particles with high QY values.

4. Conclusion

We established the sol-gel preparation method of undoped HfO_2 spherical particles, and then produced Tb^{3+} -doped HfO_2 spherical particles with green luminescence by applying this method. Spherical particles with good morphology and comparatively high dispersibility were obtained from solutions with the molar ratio $\text{SPAN85}^\circ\text{:H}_2\text{O} = 1:8\text{--}17.5$, their sizes being 0.2–5 μm in diameter. It is found that SPAN85° plays an important role in obtaining HfO_2 spherical particles without aggregation. Spherical particles heat treated at 400°C or below were amorphous, and those heat treated at 600°C or above were crystallized. Cubic HfO_2 is dominant in the spherical particles heat treated at 600°C, cubic and monoclinic HfO_2 coexist in those heat treated at 700°C, and monoclinic HfO_2 becomes dominant in those heat treated at 800°C or above. Crystallization and phase transition temperatures of $1\text{Tb}_2\text{O}_3\cdot99\text{HfO}_2$ spherical particle were slightly

lower than those of undoped spherical particle. $1\text{Tb}_2\text{O}_3\cdot99\text{HfO}_2$ spherical particle showed green luminescence due to the $^5\text{D}_4 \rightarrow ^7F_J$ ($J = 6, 5, 4, 3$) transitions of the Tb^{3+} ion. The luminescence was strong in both the $1\text{Tb}_2\text{O}_3\cdot99\text{HfO}_2$ dried gel particles ($QY = 1.3 \pm 0.1\%$) and the spherical particle heat treated at 1000°C ($QY = 0.9 \pm 0.1\%$).

References

- 1) C. Carbone, *Phys. Rev. B*, **45**, 2079–2084 (1992).
- 2) Y. Wang, M.-T. Ho, L. V. Goncharova, L. S. Wielunski, S. Rivillon-Amy, Y. J. Chabal, T. Gustafsson, N. Moumen and M. Boleslawski, *Chem. Mater.*, **19**, 3127–3138 (2007).
- 3) M. Ocana, M. Andres and C. J. Serna, *Colloid. Surface A*, **79**, 169–175 (1993).
- 4) A. Lakhlifi, Ch. Leroux, P. Satre, B. Durand, M. Roubin and G. Nihoul, *J. Solid State Chem.*, **119**, 289–298 (1995).
- 5) M. V. Ibanez, C. Le Luyer, O. Marty and J. Mugnier, *Opt. Mater.*, **24**, 51–57 (2003).
- 6) M. V. Ibanez, C. L. Luyer, C. Dujardin and J. Mugnier, *Mater. Sci. Engineer. B*, **105**, 12–15 (2003).
- 7) M. G. Hipolito, O. A. Fragoso, J. Guzman, E. Martinez and C. Falcony, *Phys. Status Solidi A*, **201**, R127–R130 (2004).
- 8) V. Kiisk, I. Sildos, S. Lange, V. Reed, T. Tatte, M. Kirm and J. Aarik, *Appl. Surf. Sci.*, **247**, 412–417 (2005).
- 9) S. Lange, V. Kiisk, V. Reed, M. Kirm, J. Aarik and I. Sildos, *Opt. Mater.*, **28**, 1238–1242 (2006).
- 10) M. G. Hipolito, U. Caldino, O. A. Fragoso, M. A. A. Perez, R. M. Martinez and C. Falcony, *Phys. Status Solidi A*, **204**, 2355–2361 (2007).
- 11) H. Toraya, M. Yoshimura and S. Sōmiya, *Commun. Am. Ceram. Soc.*, **65**, C72–C72 (1982).
- 12) M. Yoshimura and S. Sōmiya, *Mater. Chem. Phys.*, **61**, 1–8 (1999).
- 13) P. E. Meskin, F. Yu. Sharikov, V. K. Ivanov, B. R. Churagulov and Y. D. Tretyakov, *Mater. Chem. Phys.*, **104**, 439–443 (2007).
- 14) M. Ocana, M. Andres, M. Martinez, C. J. Serna and E. Matijevic, *J. Colloid. Interf. Sci.*, **163**, 262–268 (1994).
- 15) Z. J. Wang, T. Kumagai, H. Kokawa, J. Tsuaur, M. Ichiki and R. Maeda, *J. Cryst. Growth*, **281**, 452–457 (2005).
- 16) M. Modreanu, J. S. Parramon, D. O'Connell, J. Justice, O. Durand and B. Servet, *Mater. Sci. Engineer. B*, **118**, 127–131 (2005).
- 17) T. Mori, M. Fujiwara, R. R. Manory, I. Shimizu, T. Tanaka and S. Miyake, *Surf. Coat. Tech.*, **169**–**170**, 528–531 (2003).
- 18) D. Larcher, G. Sudant, R. Patrice and J. M. Tarascon, *Chem. Mater.*, **15**, 3543–3551 (2003).
- 19) M. V. Ibanez, C. L. Luyer, S. Parpla, C. Dujardin and J. Mugnier, *Opt. Mater.*, **27**, 1541–1546 (2005).
- 20) H. Hosono, T. Kinoshita, H. Kawazoe, M. Yamazaki, Y. Yamamoto and N. Sawanobori, *J. Phys. Condens. Matter*, **10**, 9541–9547 (1998).
- 21) E. Zych, P. J. Deren, W. Strek, A. Meijerink, W. Mielcarek and K. Domagala, *J. Alloy. Comp.*, **323**–**324**, 8–12 (2001).
- 22) Y. H. Wang, J. C. Zhang and X. Guo, *Electrochem. Solid-State Lett.*, **9**, H26–H29 (2006).
- 23) N. Wada, F. Ogura, K. Yamamoto and K. Kojima, *Glass Technol.*, **46**, 163–170 (2005).
- 24) K. Yamamoto, N. Tsuganezawa, S. Makimura, D. Sawa, S. Nakahigashi, K. Kojima and Y. Hasegawa, *J. Mater. Res.*, **23**, 1642–1646 (2008).
- 25) R. T. Wegh and A. Meijerink, *Phys. Rev. B*, **60**, 10820–10830 (1999).
- 26) P. Dorenbos, *J. Lumin.*, **91**, 91–106 (2000).
- 27) M. Kirm, J. Aarik, M. Jurgens and I. Sildos, *Nucl. Instrum. Method. A*, **537**, 251–255 (2005).
- 28) Y. C. Wu, C. Garapon, R. Bazzi, A. Pillonnet, O. Tillement and J. Mugnier, *Appl. Phys. A*, **87**, 697–704 (2007).